Photochemical Generation of Cyclopentadienyliron Dicarbonyl Anion by a Nicotinamide Adenine Dinucleotide Dimer Analogue

Shunichi Fukuzumi,*,† Kei Ohkubo,† Mamoru Fujitsuka,‡ Osamu Ito,‡ Marcus C. Teichmann,§ Emmanuel Maisonhaute,§ and Christian Amatore*,§

Department of Materials and Life Science, Graduate School of Engineering, Osaka University, CREST, Japan Science and Technology Corporation, Suita, Osaka 565-0871, Japan, Institute for Chemical Reaction Science, Tohoku University, CREST, Japan Science and Technology Corporation, Sendai, Miyagi 980-8577, Japan, and Département de Chimie, Ecole Normale Supérieure, UMR CNRS 8640 "Pasteur", 24 rue Lhomond, F-75231 Paris Cedex 05, France

Received August 22, 2000

Irradiation of the absorption band of an NAD (nicotinamide adenine dinucleotide) dimer analogue, 1-benzyl-1,4-dihydronicotinamide dimer, $(BNA)_2$, in acetonitrile containing a cyclopentadienyliron dicarbonyl dimer, $[CpFe(CO)_2]_2$, results in generation of 2 equiv of the cyclopentadienyliron dicarbonyl anion, $[CpFe(CO)_2]^-$, accompanied by the oxidation of $(BNA)_2$ to yield 2 equiv of BNA^+. The studies on the quantum yields, the electrochemistry, and the transient absorption spectra have revealed that the photochemical generation of $[CpFe(CO)_2]^-$ by $(BNA)_2$ proceeds via photoinduced electron transfer from the triplet excited state of $(BNA)_2$ to $[CpFe(CO)_2]_2$.

Introduction

The cyclopentadienyliron dicarbonyl anion, $[CpFe(CO)_2]^-$ ($Cp = \eta^5$-C_5H_5), has played an important role in the development of inorganic and organometallic chemistry[1−3] because it is readily alkylated, acylated, or metalated by reaction with an appropriate electrophile.[1−3] However, strong reducing reagents such as Na/Hg amalgam,[4] Na/K alloy,[5] Na dispersion,[6] and trialkylborohydrides[7] have so far been required to produce $[CpFe(CO)_2]^-$ by the chemical reductive cleavage of the cyclopentadienyliron dicarbonyl dimer, $[CpFe(CO)_2]_2$. Alternatively, $[CpFe(CO)_2]^-$ can be produced by the electrochemical reduction of $[CpFe(CO)_2]_2$ at highly negative potentials.[8,9] On the other hand, photochemistry of metal carbonyl compounds has provided a valuable synthesis technique in organometallic chemistry.[10−17] In particular, photochemistry of $[CpFe(CO)_2]_2$ has received much attention because there are a diversity of reaction pathways leading to mononuclear, dinuclear, and even ionic products.[12,15−17] Loss of CO and homolysis of the Fe−Fe bond are primary photochemical processes known for $[CpFe(CO)_2]_2$.[12−17] However, there has so far been no report on the photochemical reduction of $[CpFe(CO)_2]_2$ by an electron donor to produce $[CpFe(CO)_2]^-$.

We report herein a convenient method for generation of $[CpFe(CO)_2]^-$ by the photochemical reduction of $[CpFe(CO)_2]_2$ by a unique organic two-electron donor, that is, an NAD

* To whom correspondence should be addressed. E-mail for S.F.: fukuzumi@ap.chem.eng.osaka-u.ac.jp. E-mail for C.A.: christian.amatore@ens.fr.

† Osaka University.

‡ Tohoku University.

§ Ecole Normale Supérieure.

(1) (a) Ellis, J. E. *J. Organomet. Chem.* **1975**, *86*, 1. (b) Ellis, J. E. *Comprehensive Organic Synthesis*; Trost, B. M., Ed.; Pergamon Press: Oxford, 1991; Vol. 4.

(2) (a) King, R. B. *Adv. Organomet. Chem.* **1964**, *2*, 157. (b) King, R. B. *Acc. Chem. Res.* **1970**, *3*, 417.

(3) (a) Nitay, M.; Priester, W.; Rosenblum, M. *J. Am. Chem. Soc.* **1978**, *100*, 3620. (b) Rosenblum, M. *Acc. Chem. Res.* **1974**, *7*, 122. (c) Rosenblum, M. *J. Organomet. Chem.* **1986**, *300*, 191. (d) Davis, R.; Khazaal, N. M. S.; Maistry, V. *J. Chem. Soc., Chem. Commun.* **1986**, 1387.

(4) King, R. B. *Organometallic Synthesis*; Academic Press: New York, 1965; Vol. 1.

(5) Ellis, J. E.; Flom, E. A. *J. Organomet. Chem.* **1975**, *99*, 263.

(6) (a) Piper, T. S.; Wilkinson, G. *J. Inorg. Nucl. Chem.* **1956**, *3*, 104. (b) Fischer, E. O.; Böttcher, R. *Z. Naturforsch., B* **1955**, *10*, 600. (c) Reger, D. L.; Fauth, D. J.; Dukes, M. D. *Synth. React. Inorg. Met.−Org. Chem.* **1977**, *7*, 151.

(7) Gladysz, J. A.; Williams, G. M.; Tam, W.; Johnson, D. L.; Parker, D. W.; Selover, J. C. *Inorg. Chem.* **1979**, *18*, 553.

(8) (a) Connelly, N. G.; Geiger, W. E. *Adv. Organomet. Chem.* **1984**, *23*, 1. (b) Ferguson, J. A.; Meyer, T. J. *Inorg. Chem.* **1971**, *10*, 1025. (c) Johnson, E. C.; Meyer, T. J.; Winterton, N. *Inorg. Chem.* **1971**, *10*, 1673. (d) Pugh, J. R.; Meyer, T. J. *J. Am. Chem. Soc.* **1988**, *110*, 8245.

(9) (a) Dessy, R. E.; Weissman, P. M.; Pohl, R. L. *J. Am. Chem. Soc.* **1966**, *88*, 5117. (b) Legzdins, P.; Wassink, B. *Organometallics* **1984**, *3*, 1811. (c) Miholová, D.; Vlcek, A. A. *Inorg. Chim. Acta* **1980**, *41*, 119. (d) Morán, M.; Cuadrado, I.; Losada, J. *J. Organomet. Chem.* **1987**, *320*, 317.

(10) (a) Meyer, T. J. *Prog. Inorg. Chem.* **1975**, *19*, 1. (b) Bullock, J. P.; Palazotto, M. C.; Mann, K. R. *Inorg. Chem.* **1991**, *30*, 1284.

(11) Pugh, J. R.; Meyer, T. J. *J. Am. Chem. Soc.* **1992**, *114*, 3784.

(12) Wrighton, M. *Chem. Rev.* **1974**, *74*, 401.

(13) (a) Meyer, T. J.; Caspar, J. V. *Chem. Rev.* **1985**, *85*, 187. (b) Caspar, J. V.; Meyer, T. J. *J. Am. Chem. Soc.* **1980**, *102*, 7794.

(14) Geoffroy, G. L.; Wrighton, M. S. *Organometallic Photochemistry*; Academic Press: New York, 1979.

(15) (a) Abrahamson, H. B.; Palazzotto, M. C.; Reichel, C. L.; Wrighton, M. S. *J. Am. Chem. Soc.* **1979**, *101*, 4123. (b) Blaha, J. P.; Bursten, B. E.; Dewan, J. C.; Frankel, R. B.; Randolph, C. L.; Wilson, B. A.; Wrighton, M. S. *J. Am. Chem. Soc.* **1985**, *107*, 4561. (c) Hooker, R. H.; Mahmoud, K. A.; Rest, A. J. *J. Chem. Soc., Chem. Commun.* **1983**, 1022.

(16) (a) Bursten, B. E.; McKee, S. D.; Platz, M. *J. Am. Chem. Soc.* **1989**, *111*, 3428. (b) Zhang, S.; Brown, T. L. *J. Am. Chem. Soc.* **1993**, *115*, 1779. (c) Kvietok, F. A.; Bursten, B. E. *J. Am. Chem. Soc.* **1994**, *116*, 9807. (d) Tyler, D. R.; Schmidt, M. A.; Gray, H. B. *J. Am. Chem. Soc.* **1979**, *101*, 2753.

(17) (a) George, M. W.; Dougherty, T. P.; Heilweil, E. J. *J. Phys. Chem.* **1996**, *100*, 201. (b) Dixon, A. J.; George, M. W.; Hughes, C.; Poliakoff, M.; Turner, J. J. *J. Am. Chem. Soc.* **1992**, *114*, 1719. (c) Dixon, A. J.; Healy, M. A.; Poliakoff, M.; Turner, J. J. *J. Chem. Soc., Chem. Commun.* **1986**, 994.

10.1021/ic0009627 CCC: $20.00
Published on Web 02/13/2001

(nicotinamide adenine dinucleotide) dimer analogue 1-benzyl-1,4-dihydronicotinamide dimer [$(BNA)_2$].[18,19] Combination of the photochemical and electrochemical results obtained in this study provides confirmative bases to elucidate the reaction mechanism of the photochemical reduction of $[CpFe(CO)_2]_2$ by $(BNA)_2$.

Experimental Section

Materials. Cyclopentadienyliron dicarbonyl dimer, $[CpFe(CO)_2]_2$ ($Cp = \eta^5$-C_5H_5), was purchased from Tokyo Kasei Organic Chemicals, Japan, and from Aldrich, France, for the experiments performed in Osaka and in Paris, respectively. In both cases it was used as received. Pentamethylcyclopentadienyliron dicarbonyl dimer, $[Cp^*Fe(CO)_2]_2$ ($Cp^* = \eta^5$-C_5Me_5), was obtained from Strem Chemicals, Inc., U.S. $[CpFe(CO)_2]^-NBu_4^+$ used in the voltammetric experiments was prepared by pre-electrolysis in a two-compartment cell of a solution of $[CpFe(CO)_2]_2$ at -1.6 V vs SCE in deaerated acetonitrile in the presence of 0.3 M NBu_4BF_4. An amount of 10 mL of the electrolyzed solution was transferred with a syringe to the voltammetric cell. 1-Benzyl-1,4-dihydronicotinamide dimer [$(BNA)_2$] was prepared according to the literature.[20] Acetonitrile (MeCN) used as a solvent was purified and dried according to the standard procedure.[21]

Reaction Procedure. Typically, $[CpFe(CO)_2]_2$ (1.0×10^{-3} M) and $(BNA)_2$ (1.0×10^{-3} M) were added to an NMR tube that contained deaerated CD_3CN solution (0.60 cm^3) under an atmospheric pressure of argon and the solution was irradiated with a Xe lamp (Ushio model V1-501C) through a UV cut-off filter (Toshiba UV-31) transmitting $\lambda > 300$ nm at 298 K for 30 min. The reaction products of $[CpFe(CO)_2]_2$ and $[Cp^*Fe(CO)_2]_2$ with $(BNA)_2$ were identified by the ^{1}H NMR spectra by comparing them with those of authentic samples. The ^{1}H NMR measurements were performed using a JNM-GSX-400 (400 MHz) NMR spectrometer. ^{1}H NMR (CD_3CN): $[CpFe(CO)_2]^-$ δ (Me_4Si, ppm), 4.16 (s, 5H); $[Cp^*Fe(CO)_2]^-$, δ 1.79 (s, 15H); BNA^+, δ 5.76 (s, 2H), 7.49 (m, 5H), 8.11 (t, 1H, $J = 6.8$ Hz), 8.80 (m 2H,), 9.16 (s, 1H).

Quantum Yield Determinations. A standard actinometer (potassium ferrioxalate)[22] was used for the quantum yield determination of the photoreduction of $[CpFe(CO)_2]_2$ by $(BNA)_2$. Square quartz cuvettes (10 mm i.d.), which contained a deaerated MeCN solution (3.0 cm^3) of $(BNA)_2$ (5.6×10^{-4} M) together with $[CpFe(CO)_2]_2$ at various concentrations, were irradiated with monochromatized light of $\lambda = 350$ nm from a Shimadzu RF-5000 fluorescence spectrophotometer. Under the conditions of actinometry experiments, the actinometer and $(BNA)_2$ absorbed essentially all the incident light of $\lambda = 350$ nm. The light intensity of monochromatized light of $\lambda = 350$ nm was determined as 2.32×10^{-9} einstein s^{-1} with a slit width of 20 nm. The photochemical reaction was monitored using a Hewlett-Packard 8452A diode-array spectrophotometer. The quantum yields were determined from an increase in absorbance due to the cyclopentadienyliron dicarbonyl anion, $[CpFe(CO)_2]^-$. To avoid the contribution of light absorption of the products, only the initial rates were determined for determination of the quantum yields.

Cyclic Voltammetry. Cyclic voltammetry measurements were performed with a homemade potentiostat[23] and a waveform generator, PAR model 175. The fast-scan cyclic voltammograms were recorded with a Nicolet 3091 digital oscilloscope. The one-compartment electrochemical cell was of airtight design with high-vacuum glass stopcock fitted with either Teflon or Kalretz (Du Pont) O-rings in order to prevent contamination by grease. The connections to the high-vacuum line and to the Schlenck containing the solvent were obtained by spherical joints also fitted with Kalretz O-rings. The working electrode was a homemade platinum disk microelectrode of 10 μm radius.[24] The counter electrode consisted of a platinum spiral, and the quasi-reference electrode was a silver spiral. The quasi-reference electrode drift was negligible for the time required by a single experiment. Both the counter and the reference electrodes were separated from the working electrode by ~0.5 cm. Potentials were measured with ferrocene standard and are always referenced to SCE. $E_{1/2}$ values correspond to $(E_{pc} + E_{pa})/2$ from CV curves. Ferrocene was also used as an internal standard for checking the electrochemical reversibility of a redox couple.

Fluorescence Quenching. Fluorescence measurements were carried out on a Shimadzu RF-5000 spectrofluorophotometer. The solution was deoxygenated by argon purging for 10 min prior to the measurements. The fluorescence decay of $(BNA)_2$ was measured using a Horiba NAES-1100 time-resolved spectrofluorophotometer.

Laser Flash Photolysis. The measurements of transient absorption spectra of $^3[(BNA)_2]^*$ in the presence of $[CpFe(CO)_2]_2$ were performed according to the following procedures. The $(BNA)_2$ solution (1.0×10^{-3} M) was excited by a Nd:YAG laser (Quanta-Ray, GCR-130, 6 ns fwhm) at 350 nm with a power of 7 mJ. A pulsed Xenon flash lamp (Tokyo Instruments, XF80-60, 15 J, 60 ms fwhm) was used for the probe beam, which was detected with a Si−PIN photodiode (Hamamatsu G5125-10) after passing through the photochemical quartz vessel (10 mm × 10 mm) and a monochromator. The output from Si−PIN photodiode was recorded with a digitizing oscilloscope (HP 54510B, 300 MHz). Since the solution of $(BNA)_2$ in acetonitrile disappeared by each laser shot (350 nm; 7 mJ) in the presence of $[CpFe(CO)_2]_2$, the transient spectra were recorded using fresh solutions for each laser excitation. All experiments were performed at 298 K. The solution was deoxygenated by argon purging for 10 min prior to the measurements.

ESR Measurements. ESR spectra of the photolyzed MeCN solution of $[CpFe(CO)_2]_2$ (5.0×10^{-4} M) and $(BNA)_2$ (5.0×10^{-4} M) were taken on a JEOL JES-RE1XE and were recorded under nonsaturating microwave power conditions. A sample solution was irradiated by using a high-pressure mercury lamp (USH-1005D) focusing at the sample cell in the ESR cavity. The magnitude of modulation was chosen to optimize the resolution and signal-to-noise (S/N) ratio of the observed spectra. The g values were calibrated using a Mn^{2+} marker.

Theoretical Calculations. Density functional calculations were performed on a Compaq DS20E computer using the Amsterdam density functional (ADF) program, version 1999.02, developed by Baerends et al.[25] The electronic configurations of the molecular systems were described by an uncontracted triple-ζ Slater-type orbital basis set (ADF basis set IV) with a single polarization function used for each atom. Core orbitals were frozen through 1s (C, O) and 3p (Fe). The calculations were performed using the local exchange−correlation potential by Vosko et al.[26] and the nonlocal gradient corrections by Becke[27] and Perdew[28] during the geometry optimizations. First-order scalar relativistic correlations were added to the total energy. Final geometries and energetics were optimized by using the algorithm of Versluis and Ziegler[29] provided in the ADF package and were considered converged when the changes in bond lengths between subsequent iterations fell below 0.01 Å.

Results and Discussion

Photoreduction of $[CpFe(CO)_2]_2$. Irradiation of an acetonitrile (MeCN) solution containing $(BNA)_2$ (7.0×10^{-5} M, $\lambda_{max} = 350$ nm) and $[CpFe(CO)_2]_2$ (7.0×10^{-5} M) with UV−visible light ($\lambda = 350$ nm) results in the disappearance of absorbance due to $[CpFe(CO)_2]_2$ and $(BNA)_2$ accompanied by the appearance of a new broad absorption band at ca. $\lambda = 450$ nm with

(18) Patz, M.; Kuwahara, Y.; Suenobu, T.; Fukuzumi, S. *Chem. Lett.* **1997**, 567.
(19) Fukuzumi, S.; Suenobu, T.; Patz, M.; Hirasaka, T.; Itoh, S.; Fujitsuka, M.; Ito, O. *J. Am. Chem. Soc.* **1998**, *120*, 8060.
(20) Wallenfels, K.; Gellrich, M. *Chem. Ber.* **1959**, *92*, 1406.
(21) Perrin, D. D.; Armarego, W. L. F. *Purification of Laboratory Chemicals*; Butterworth-Heinemann: Oxford, 1988.
(22) Hatchard, C. G.; Parker, C. A. *Proc. R. Soc. London, Ser. A* **1956**, *235*, 518.
(23) Amatore, C.; Lefrou, C.; Pflüger, F. *J. Electroanal. Chem.* **1989**, *270*, 43.
(24) Amatore, C.; Thouin, L.; Bento, M. F. *J. Electroanal. Chem.* **1999**, *463*, 45.
(25) (a) Baerends, E. J.; Ellis, D. E.; Ros, P. *Chem. Phys.* **1973**, *2*, 41. (b) te Velde, G.; Baerends, E. J. *J. Comput. Phys.* **1992**, *99*, 84.
(26) Vosko, S. H.; Wilk, L.; Nusair, M. *Can. J. Phys.* **1980**, *58*, 1200.
(27) Becke, A. *Phys. Rev. A* **1988**, *38*, 3098.
(28) (a) Perdew, J. P. *Phys. Rev. B* **1986**, *33*, 8822. (b) Perdew, J. P. *Phys. Rev. B* **1986**, *34*, 7406.
(29) Versluis, L.; Ziegler, T. *J. Chem. Phys.* **1988**, *88*, 322.

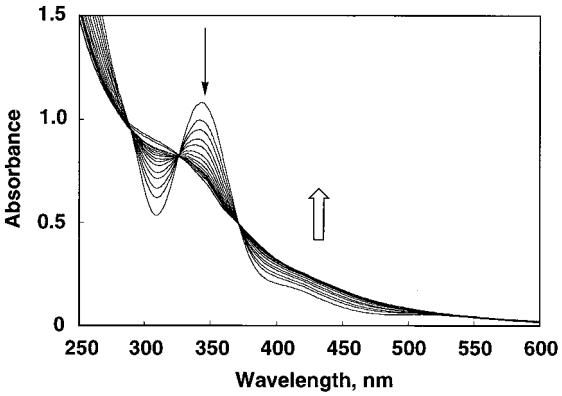

Figure 1. Electronic absorption spectra observed in the photochemical reaction of $[CpFe(CO)_2]_2$ (7.0×10^{-5} M) with $(BNA)_2$ (7.0×10^{-5} M) in deaerated MeCN at 298 K.

clean isosbestic points as shown in Figure 1. The oxidation and reduction products of $(BNA)_2$ and $[CpFe(CO)_2]_2$ were identified as BNA^+ and $[CpFe(CO)_2]^-$ by the ^1H NMR spectra of the product solution, respectively (see Experimental Section). Thus, the stoichiometry of the photochemical reaction is given by eq 1, where $[CpFe(CO)_2]_2$ is known to exist predominantly as a

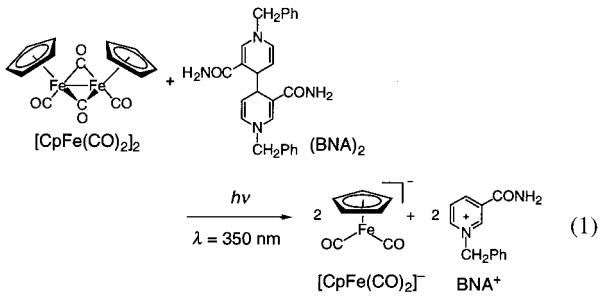

(1)

cis isomer in the two-carbonyl bridged form.[30−32] When $[CpFe(CO)_2]_2$ was replaced by the pentamethylcyclopentadienyliron dicarbonyl dimer, $[Cp^*Fe(CO)_2]_2$ ($Cp^* = \eta^5$-C_5Me_5), the photoreduction of $[Cp^*Fe(CO)_2]_2$ by $(BNA)_2$ hardly occurred.

The irradiation with light of λ_{max} of $(BNA)_2$ is essential for the selective formation of $[CpFe(CO)_2]^-$ without loss of CO. The quantum yield of the photogeneration of $[CpFe(CO)_2]^-$ was determined from an increase in absorbance due to $[CpFe(CO)_2]^-$ under irradiation with light at $\lambda = 350$ nm. The quantum yield (Φ) increased with an increase in the $[CpFe(CO)_2]_2$ concentration to approach a limiting value (Φ_∞), as shown in Figure 2a. Such a saturated dependence of Φ on the $[CpFe(CO)_2]_2$ concentration is expressed by

$$\Phi = \frac{\Phi_\infty K_{obs}[Fp_2]}{1 + K_{obs}[Fp_2]} \qquad (2)$$

where Fp_2 denotes $[CpFe(CO)_2]_2$ and K_{obs} is the quenching constant that can be converted to the corresponding rate constant (k_{obs}) provided that the lifetime of the excited state involved in the reaction (τ) is known: $k_{obs} = K_{obs}\tau^{-1}$. Equation 2 is rewritten as

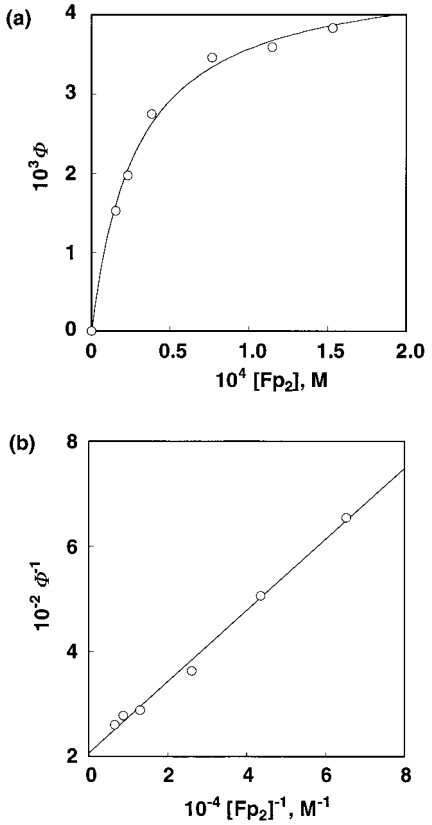

Figure 2. (a) Dependence of the quantum yield (Φ) on $[Fp_2]$ for the photoreduction of $[CpFe(CO)_2]_2$ (Fp_2) by $(BNA)_2$ (5.6×10^{-5} M) in deaerated MeCN at 298 K. (b) Plot of Φ^{-1} vs $[Fp_2]^{-1}$.

$$\Phi^{-1} = \Phi_\infty{}^{-1}[1 + (K_{obs}[Fp_2])^{-1}] \qquad (3)$$

and the linear plot of Φ^{-1} vs $[Fp_2]^{-1}$ is shown in Figure 2b. From the slope and intercept are obtained the Φ_∞ and K_{obs} values as 4.8×10^{-3} and 3.3×10^4 M^{-1}.

Irradiation of the absorption band ($\lambda_{max} = 350$ nm) of $(BNA)_2$ results in fluorescence ($\lambda_{max} = 390$ nm). From these values is obtained the excitation energy as 3.36 eV. Since the one-electron oxidation potential (E^0_{ox}) of $(BNA)_2$ is 0.26 V (vs SCE),[18] the E^0_{ox} value of the singlet excited state [$^1(BNA)_2$*] is determined as -3.1 V by subtracting the excitation energy from the E^0_{ox} value of the ground state. On the other hand, a fast-scan cyclic voltammetry was used to determine the one-electron reduction potential (E^0_{red}) of $[CpFe(CO)_2]_2$ in MeCN at 298 K. Slow-scan voltammograms of $[CpFe(CO)_2]_2$ at temperatures above 248 K have been reported to show an irreversible reduction wave due to the instability of an initially produced dimer radical anion $[CpFe(CO)_2]_2^{\bullet-}$, which dissociates into a mononuclear anion, $[CpFe(CO)_2]^-$, and a further reducible radical, $[CpFe(CO)_2]^\bullet$,

$$[CpFe(CO)_2]_2^{\bullet-} \rightarrow [CpFe(CO)_2]^\bullet + [CpFe(CO)_2]^- \qquad (4)$$

resulting in a net two-electron reduction.[9,33,34] As the temperature is lowered, the reduction of $[CpFe(CO)_2]_2$ becomes reversible.[34]

Electrochemical Oxidation of $[CpFe(CO)_2]^-$. At moderate scan rates ($v < 10^2$ V s^{-1}) the steady-state limit of the voltammetric pattern obtained upon continuous cycling between -0.42 and -2.1 V vs SCE on a bulk solution of $[CpFe(CO)_2]^-$

(30) Hepp, A. F.; Blaha, J. P.; Lewis, C.; Wrighton, M. S. *Organometallics* **1984**, *3*, 174.
(31) Bullitt, J. G.; Cotton, F. A.; Marks, T. J. *J. Am. Chem. Soc.* **1970**, *92*, 2155.
(32) Adams, R. D.; Cotton, F. A. *J. Am. Chem. Soc.* **1973**, *95*, 6589.
(33) Davies, S. G.; Simpson, S. J.; Parker, V. D. *J. Chem. Soc., Chem. Commun.* **1984**, 352.
(34) Dalton, E. F.; Ching, S.; Murray, R. W. *Inorg. Chem.* **1991**, *30*, 2642.

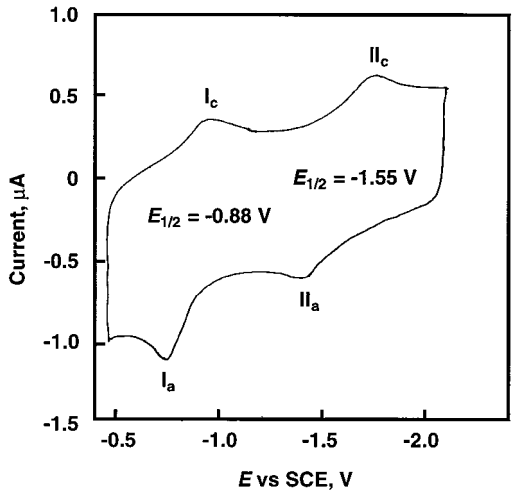

Figure 3. Cyclic voltammogram for the oxidation of the monomer anion $[CpFe(CO)_2]^-$ (3.1×10^{-3} M) in deaerated MeCN containing Bu_4NBF_4 with Pt electrode at 298 K. Sweep rate is 3280 V s^{-1}.

exhibits two major waves as reported previously.[34,35] One, wave I_a, is anodic and features the one-electron oxidation of $[CpFe(CO)_2]^-$ at ca. −0.75 V vs SCE.[33,34] The other, wave II_c of approximately equal current intensity, is observed around ca. −1.75 V vs SCE and features the reduction of the $[CpFe(CO)_2]_2$ dimer as evidenced by comparison with an authentic sample. This pattern confirms that the radical $[CpFe(CO)_2]^\bullet$ formed upon the one-electron oxidation of $[CpFe(CO)_2]^-$ at wave I_a undergoes a fast dimerization to afford $[CpFe(CO)_2]_2$ that is then reduced through an overall two-electron reduction at wave II_c to regenerate the parent anion, thus giving rise to the impression of the occurrence of a reversible couple with a large peak-to-peak separation (ca. 1 V).

Besides the facts that both peak potentials experience displacements with the scan rate (ca. −20 mV per log v for wave I_a, and ca. −30 mV per log v for wave II_c) and that the peak of wave I_a depends on the concentration of $[CpFe(CO)_2]^\bullet$ (ca. −20 mV per log C), further evidence that the system I_a/II_c is not a canonical reversible couple is given by the growth of a reversible anodic wave, II_a, coupled to wave II_c, as soon as the scan rate is increased above a few 10^2 V s^{-1}. Above a few kV s^{-1}, wave II_a has a peak current intensity comparable to that of wave II_c, showing that a full reversible behavior is achieved for the redox couple $[CpFe(CO)_2]_2/[CpFe(CO)_2]_2^{\bullet-}$ as shown in Figure 3. This allows the determination of the rate constant $k_c \approx 5 \times 10^2$ s^{-1} of the Fe−Fe bond cleavage in $[CpFe(CO)_2]_2^{\bullet-}$, as well as of the standard reduction potential of $[CpFe(CO)_2]_2$ at $E_{1/2} = -1.55$ V vs SCE.

When the scan rate approaches the kV s^{-1} range, a second cathodic wave (I_c) develops, being apparently the anodic counterpart of wave I_a. The growth of this wave upon increasing scan rate is concomitant with a comparable decay of the system of waves II_c/II_a, showing that the species reduced at wave I_c is an intermediate on the way to $[CpFe(CO)_2]_2$. At $v \approx 3$ kV s^{-1} (Figure 3), the peak current intensity of wave I_c is approximately equal to those of waves II_c and II_a. This establishes that the intermediate reduced at wave I_c has a half-lifetime of ca. 140 μs. Such voltammetric behavior would suggest that this intermediate is the $[CpFe(CO)_2]^\bullet$ radical formed upon the one-electron oxidation of $[CpFe(CO)_2]^-$ at wave I_a. However, this interpretation must be ruled out because this radical is reported

Scheme 1

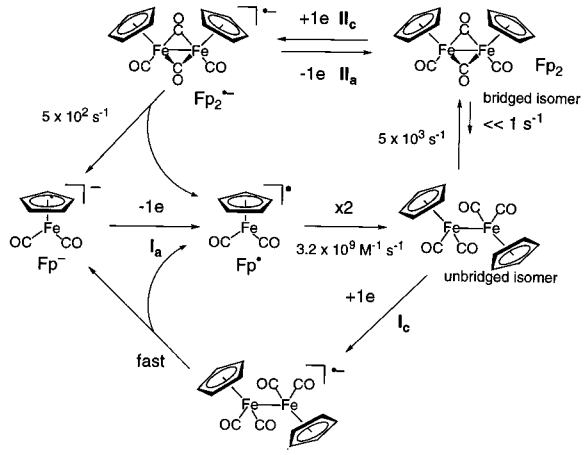

to dimerize with a rate constant of 3.2×10^9 M^{-1} s^{-1},[13] so intercepting its fast dimerization under the millimolar conditions used here would require scan rates ca. 100 times larger than that used in Figure 3.[35] Moreover, if the $[CpFe(CO)_2]^\bullet$ radical were detected under the conditions of Figure 3, its ESR spectrum would be observable under irradiation of a mixture of $(BNA)_2$ and $[CpFe(CO)_2]_2$ (vide infra) with an intensity being approximately 20% that of $[CpFe(CO)_2]_2^{\bullet-}$ based on their relative lifetimes. Such an ESR signal is not observed (vide infra), which points to a much larger reaction rate for $[CpFe(CO)_2]^\bullet$, in agreement with a previous report.[13] Henceforth, under the conditions used in Figure 3, the $[CpFe(CO)_2]^\bullet$ radical must undergo a quantitative dimerization and none can be reduced at wave I_c. This indicates that the species detected at wave I_c is an intermediate on the way to $[CpFe(CO)_2]_2$ in which the Fe−Fe bond is already made.

In fact, $[CpFe(CO)_2]_2$ is known to predominantly exist not only in the stable two-carbonyl bridged form but also in a less stable unbridged form.[30−32] With the unbridged form having a significantly weaker Fe−Fe bond than the bridged form, it is reasonable for such species to be reducible at a much lesser negative potential than its more stable $[CpFe(CO)_2]_2$ isomer (note that the peak potential separation between waves I_c and II_c is ca. 0.8 V). Furthermore, its one-electron reduction at wave I_c should produce a more unstable anion radical than $[CpFe(CO)_2]_2^{\bullet-}$ that is detected at wave II_a, so its reduction should regenerate its parent anion $[CpFe(CO)_2]^-$ more quickly than that of the more stable $[CpFe(CO)_2]_2$ isomer. In other words, although it is impossible for us to further characterize this species, it seems highly probable that this species detected by its reduction at wave I_c is the unbridged dimer and that the 140 μs half-lifetime corresponds to the bridging rate constant (5×10^3 s^{-1}) of the two carbonyl ligands as shown in Scheme 1.

When an authentic sample of the stable $[CpFe(CO)_2]_2$ isomer is reduced voltammetrically, the existence of the equilibrium between the unbridged and bridged isomers in Scheme 1[30−32] should lead to a CE sequence as soon as the electrode potential reaches wave I_c. Therefore, $[CpFe(CO)_2]_2$ could be reduced via the continuous displacement of the equilibrium (Scheme 1) to the side of the unbridged isomer owing to the consumption of the unbridged isomer at wave I_c, unless the backward rate constant is too small.[36] We did not observe any evidence of such a behavior even for the smallest scan rates used in this

(35) Amatore, C.; Jutand, A.; Pflüger, F. *J. Electroanal. Chem.* **1987**, *218*, 361.

(36) Bard, A. J.; Faulkner, L. R. *Electrochemical Methods*; J. Wiley & Sons: New York, 1980.

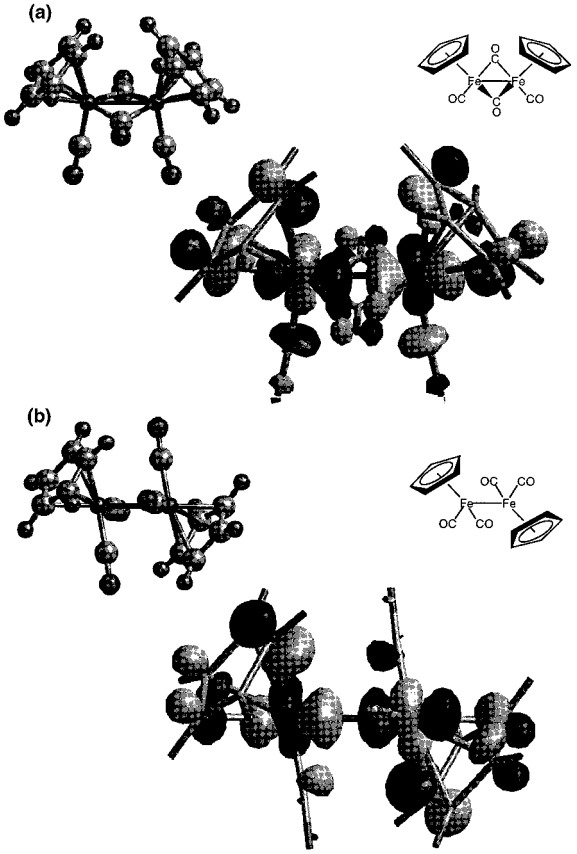

Figure 4. Ball and stick diagrams of the optimized structures of (a) the bridged and (b) unbridged isomers of $[CpFe(CO)_2]_2$ and the LUMO orbitals.

study (50 mV s^{-1}). Therefore, the backward rate constant of equilibrium (Scheme 1) has to be much less than 1 s^{-1}. Henceforth, the equilibrium constant of CO bridging has to be much larger than 5×10^3 (viz., $\Delta G° < -5.0$ kcal mol^{-1}). Within this guideline, the $E_{1/2} = -0.88$ V vs SCE deduced from the half-sum of the peak potentials of waves I_a and I_c does not correspond at all to the standard oxidation potential of $[CpFe(CO)_2]^•$ but to a kinetic potential corresponding to the pseudoreversible sequence in Scheme 1.

The thermodynamic stabilities of the bridged and unbridged isomers of $[CpFe(CO)_2]_2$ were evaluated by the Amsterdam density functional (ADF) calculations (see Experimental Section).[25−29] The final geometries and energetics were obtained by optimizing the total molecular energy with respect to all structural variables as shown in Figure 4. Consistent with the above estimation of the $\Delta G°$ value (< -5.0 kcal mol^{-1}), we find that the bridged isomer is more stable than the unbridged trans isomer by 12.3 kcal mol^{-1}. The unbridged cis isomer is less stable than the unbridged trans isomer by 13.7 kcal mol^{-1}. The LUMO (lowest unoccupied molecular orbital) of the unbridged isomer consists of the Fe−Fe σ antibonding orbital, whereas the LUMO of the bridged isomer involves the Fe−CO d−π* bonding orbital. This may be the reason for the facile cleavage of the Fe−Fe bond of the unbridged isomer upon the one-electron reduction (Scheme 1).

Mechanism of Photoreduction of $[CpFe(CO)_2]_2$ by $(BNA)_2$. Judging from the one-electron redox potentials of $^1(BNA)_2$* ($E^0_{ox} = -3.10$ V) and $[CpFe(CO)_2]_2$ ($E^0_{red} = -1.55$ V), the photoinduced electron transfer from $^1(BNA)_2$* to $[CpFe(CO)_2]_2$ is highly exergonic because the free energy change of electron transfer (ΔG^0_{et}) is −1.55 eV.

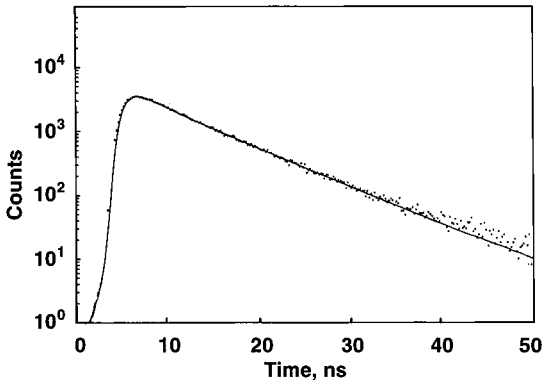

Figure 5. Fluorescence decay of $(BNA)_2$ (1.0×10^{-4} M) at $\lambda = 390$ nm in deaerated MeCN at 298 K.

The fluorescence decay of $^1(BNA)_2$* obeys first-order kinetics as shown in Figure 5. The fluorescence lifetime was determined as 7.4 ns. If the singlet excited state $^1(BNA)_2$* is responsible for the photoreduction of $[CpFe(CO)_2]_2$ by $(BNA)_2$, the K_{obs} value (3.3×10^4 M^{-1}) obtained from saturated dependence of Φ on $[Fp_2]$ (Figure 2) would be converted to the corresponding rate constant ($k_{obs} = 4.5 \times 10^{12}$ M^{-1} s^{-1}) using the relation, $k_{obs} = K_{obs}\tau^{-1}$ and $\tau = 7.4$ ns. The estimated k_{obs} value is much larger than the diffusion-limited value (2.0×10^{10} M^{-1} s^{-1}).[37] This indicates that the excited state involved in the photoreduction of $[CpFe(CO)_2]_2$ by $(BNA)_2$ should have a much longer lifetime than the singlet excited state, and therefore, it may be the triplet excited state of $(BNA)_2$.

The existence of the triplet excited state of $(BNA)_2$ is shown by the laser flash photolysis of an MeCN solution of $(BNA)_2$ with 355 nm laser light. The result is shown in Figure 6a where a new absorption band at 430 nm, which is attributed to the triplet−triplet (T−T) absorption of the triplet excited state [$^3(BNA)_2$*], is observed upon laser excitation. The T−T absorption decays obeying first-order kinetics as shown in Figure 6b. The triplet lifetime is determined as $\tau_T = 20$ μs.

In the presence of $[CpFe(CO)_2]_2$, the T−T absorption observed at 0.25 μs after laser excitation ($\lambda_{max} = 430$ nm) is changed to a new transient absorption band at 2.5 μs ($\lambda_{max} = 470$ nm), which may be attributed to $[CpFe(CO)_2]_2^{•-}$ produced by photoinduced electron transfer from $^3(BNA)_2$* to $[CpFe(CO)_2]_2$ as shown in Figure 7a. On the other hand, the oxidized product of $(BNA)_2$ [$(BNA)_2^{•+}$] is known to be converted to $BNA^•$ and BNA^+ via facile C−C bond cleavage.[18,19] Since the transient absorption spectrum of $NAD^•$ was reported to appear at $\lambda_{max} = 500$ nm,[38] the absorption spectrum of $BNA^•$ may be overlapped with that of $[CpFe(CO)_2]_2^{•-}$ at 470 nm. An increase in absorbance due to $[CpFe(CO)_2]_2^{•-}$ at 470 nm obeys pseudo-first-order kinetics as shown in Figure 6b and the pseudo-first-order rate constant increases linearly with increasing the $[CpFe(CO)_2]_2$ concentration. From the slope of a linear correlation of the pseudo-first-order rate constant vs the $[CpFe(CO)_2]_2$ concentration is obtained the rate constant (k_{et}) of photoinduced electron transfer from $^3(BNA)_2$* to $[CpFe(CO)_2]_2$ as 1.8×10^9 M^{-1} s^{-1}. On the other hand, the K_{obs} value (3.3×10^4 M^{-1}) obtained from the saturated dependence of Φ on $[Fp_2]$ (Figure 2) is converted to the corresponding rate constant ($k_{obs} = 1.6 \times 10^9$ M^{-1} s^{-1}) provided that the triplet excited state $^3(BNA)_2$* is responsible for the photoreduction of $[CpFe(CO)_2]_2$

(37) Rehm, A.; Weller, A. *Isr. J. Chem.* **1970**, *8*, 259.
(38) (a) Czochralska, B.; Lindqvist, L. *Chem. Phys. Lett.* **1983**, *101*, 297. (b) Lindqvist, L.; Czochralska, B.; Grigorov, I. *Chem. Phys. Lett.* **1985**, *119*, 494.

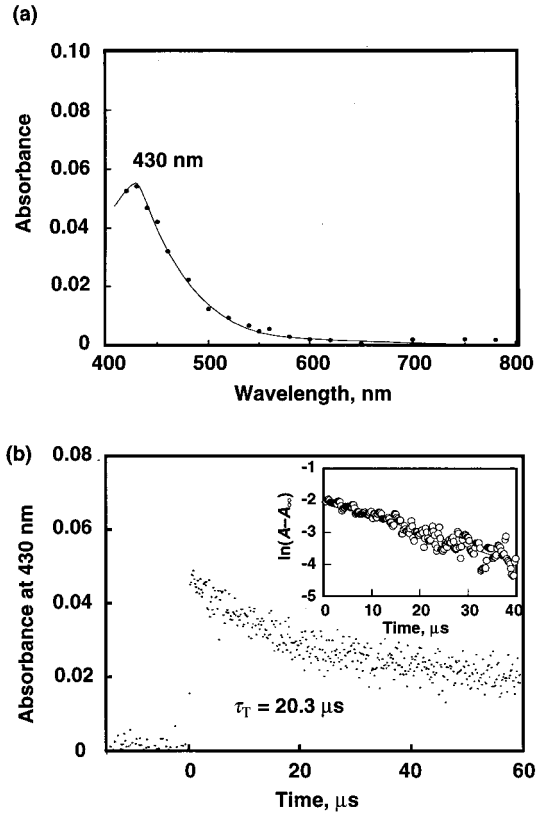

Figure 6. (a) T−T absorption spectrum of $(BNA)_2$ (1.0×10^{-3} M) obtained by the laser flash photolysis in deaerated MeCN at 298 K. (b) Kinetic trace for the T−T absorption at 430 nm in deaerated MeCN. Inset: first-order plot.

by $(BNA)_2$, using the relation $k_{obs} = K_{obs}\tau_T^{-1}$ and $\tau_T = 20$ μs. This k_{obs} value agrees with the k_{et} value (1.8×10^9 M^{-1} s^{-1}) determined directly from the appearance of the transient absorption at 470 nm due to $[CpFe(CO)_2]_2^{\bullet-}$ (Figure 7a). Such an agreement strongly indicates that the photoreduction of $[CpFe(CO)_2]_2$ by $(BNA)_2$ proceeds via photoinduced electron transfer from $^3(BNA)_2$* to $[CpFe(CO)_2]_2$.

The Fe−Fe bond of $[CpFe(CO)_2]_2^{\bullet-}$ generated in photoinduced electron transfer from $^3(BNA)_2$* to $[CpFe(CO)_2]_2$ is cleaved to give $[CpFe(CO)_2]^{\bullet}$ and $[CpFe(CO)_2]^-$ (Scheme 1).[33,34] However, the cleavage rate is relatively slow as estimated by the electrochemical measurements (Scheme 1).[33,34] In such a case $[CpFe(CO)_2]_2^{\bullet-}$ may be stable enough to be detected by ESR at a low temperature. In fact, a broad isotropic ESR signal ($g = 2.0073$) is detected under photoirradiation of an MeCN solution of $(BNA)_2$ (5.0×10^{-4} M) and $[CpFe(CO)_2]_2$ (5.0×10^{-4} M) with a high-pressure mercury lamp at 243 K as shown in Figure 8. When the temperature is lowered to 173 K, the isotropic signal is changed to the anisotropic signal in a frozen medium with $g_1 = 2.0554$, $g_2 = 2.0031$, and $g_3 = 1.9635$. The averaged value (2.0073) agrees with the isotropic value in solution. The ESR spectrum with a g value of 2.0073, which is much larger than the free spin value, may be attributed to $[CpFe(CO)_2]_2^{\bullet-}$. No organic radicals such as $BNA^{\bullet}$ was detected probably because of the fast dimerization.[19,39] In such a case it is unlikely that $[CpFe(CO)_2]^{\bullet}$ is detected by ESR because dimerization of $[CpFe(CO)_2]^{\bullet}$ is known to be as rapid as that of $BNA^{\bullet}$.[13,19]

On the basis of the above results, the reaction mechanism of the photoreduction of $[CpFe(CO)_2]_2$ by $(BNA)_2$ is summarized as shown in Scheme 2. The triplet excited state $^3(BNA)_2$* generated by intersystem crossing (ISC) upon photoexcitation of $(BNA)_2$ is quenched by electron transfer to $[CpFe(CO)_2]_2$ to give the radical ion pair in competition with the decay to the ground state.[40] The C−C bond of $(BNA)_2^{\bullet+}$ is readily cleaved to produce $BNA^{\bullet}$ and BNA^+. In the case of the photoinduced electron transfer from $(BNA)_2$ to C_{70}, the C−C bond cleavage

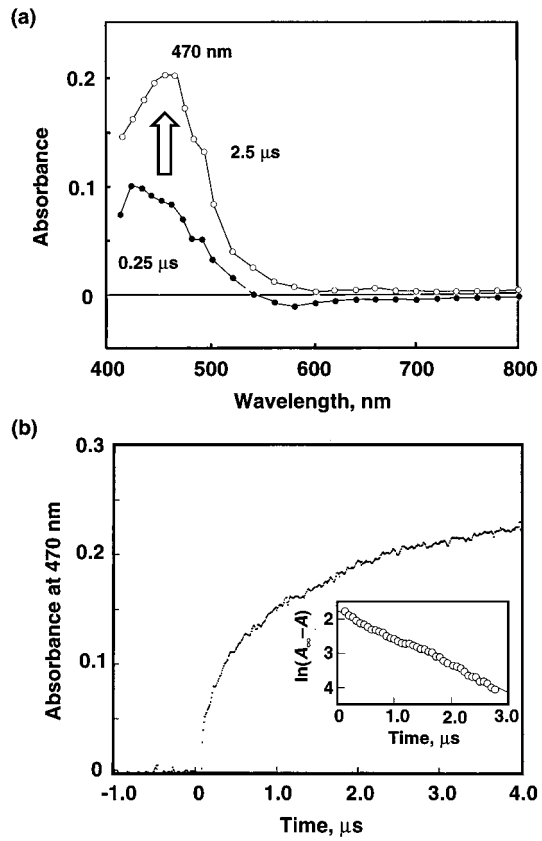

Figure 7. (a) Transient absorption spectra observed in the photoreduction of $[CpFe(CO)_2]_2$ (3.0×10^{-4} M) by $(BNA)_2$ (1.0×10^{-3} M) after laser excitation in deaerated MeCN at 298 K. (b) Kinetic trace for formation of $[CpFe(CO)_2]_2^{\bullet-}$. Inset: first-order plot.

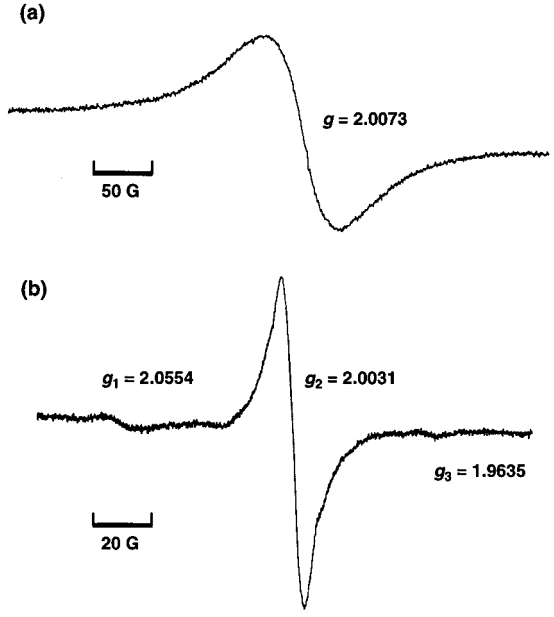

Figure 8. ESR spectra of $[CpFe(CO)_2]_2^{\bullet-}$ observed under irradiation of a deaerated MeCN solution containing $(BNA)_2$ (5.0×10^{-4} M) and $[CpFe(CO)_2]_2$ (5.0×10^{-4} M) (a) at 243 K and (b) at 173 K (frozen).

(39) Fukuzumi, S.; Koumitsu, S.; Hironaka, K.; Tanaka, T. *J. Am. Chem. Soc.* **1987**, *109*, 305.

Scheme 2

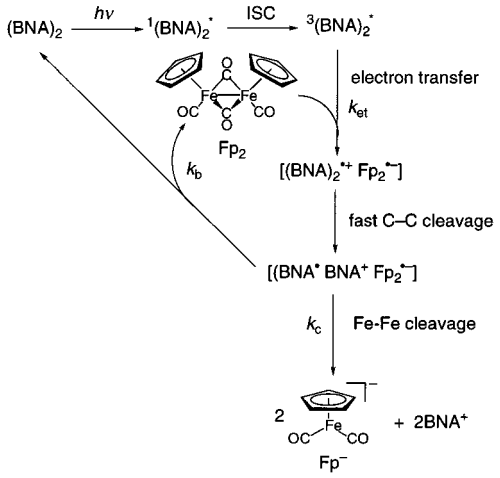

of $(BNA)_2^{\bullet+}$ is reported to be much faster than the back electron transfer from $C_{70}^{\bullet-}$ to $(BNA)_2^{\bullet+}$, leading to formation of the products with 100% quantum efficiency.[41] In the present case as well, the photoinduced electron transfer from $^3(BNA)_2$* to $[CpFe(CO)_2]_2$ results in formation of $BNA^{\bullet}$, BNA^+, and $[CpFe(CO)_2]_2^{\bullet-}$. Since the E^0_{red} value of BNA^+ (−1.08 V vs SCE)[39] is less negative than the E^0_{ox} value of $[CpFe(CO)_2]_2^{\bullet-}$ (−1.55 V), back electron transfer from $[CpFe(CO)_2]_2^{\bullet-}$ to BNA^+ (ΔG^0_{et} = 0.47 eV) may occur to regenerate $[CpFe(CO)_2]_2$ accompanied by formation of $BNA^{\bullet}$, which dimerized to reproduce $(BNA)_2$. In competition with such a back electron transfer process (k_b), the Fe−Fe bond cleavage (k_c) occurs to give $[CpFe(CO)_2]^-$ and $[CpFe(CO)_2]^{\bullet}$.[42] The electron transfer from $BNA^{\bullet}$ to $[CpFe(CO)_2]^{\bullet}$ gives BNA^+ and $[CpFe(CO)_2]^-$. Thus, the net reaction is two-electron reduction of $[CpFe(CO)_2]_2$ by $(BNA)_2$ to yield 2 equiv of $[CpFe(CO)_2]^-$ and BNA^+ (Scheme 2).

By application of the steady-state approximation to the reactive intermediates in Scheme 2, the dependence of quantum yields on the substrate concentration $[Fp_2]$ is derived as shown in

$$\Phi = \frac{[k_c/(k_c + k_b)]k_{et}\tau_T[Fp_2]}{1 + k_{et}\tau_T[Fp_2]} \quad (5)$$

which agrees with the experimental observation in eq 2. The efficiency for the photochemical reaction is thereby determined by the Fe−Fe bond cleavage rate in competition with the back electron transfer from $[CpFe(CO)_2]_2^{\bullet-}$ to BNA^+, which may be diffusion-limited judging from the highly negative ΔG^0_{et} value of the electron transfer (vide supra).[43] In the case of $[Cp^*Fe(CO)_2]_2$, the Fe−Fe bond cleavage rate in the radical anion is known to be 2 orders of magnitude slower compared to the cleavage rate of $[CpFe(CO)_2]_2$.[34] This may be the reason that the photoreduction of $[Cp^*Fe(CO)_2]_2$ by $(BNA)_2$ hardly occurred (vide supra).

In conclusion, this study provides a new method for photogeneration of $[CpFe(CO)_2]^-$ by a unique organic two-electron donor $[(BNA)_2]$ via photoinduced electron transfer from $^3(BNA)_2$* to $[CpFe(CO)_2]_2$ followed by Fe−Fe bond cleavage in $[CpFe(CO)_2]_2^{\bullet-}$.

Acknowledgment. This work was partially supported by a Grant-in-Aid for Scientific Research Priority Area (No. 11228205) from Ministry of Education, Science, Sports and Culture, Japan. This work was also supported in part by CNRS (UMR 8640 "PASTEUR"), Ecole Normale Supérieure, and the French Ministry of Research. M.C.T. welcomes the award of a Marie Curie doctoral grant by the European Community.

IC0009627

(40) Under our experimental conditions, irradiation at 350 nm results in mostly formation of $^3(BNA)_2$*, and the photocleavage of the Fe−CO bond of $[CpFe(CO)_2]_2$ is negligible on the basis of the stoichiometry of the photochemical reaction (see Experimental Section).

(41) Fukuzumi, S.; Suenobu, T.; Hirasaka, T.; Sakurada, N.; Arakawa, R.; Fujitsuka, M.; Ito, O. *J. Phys. Chem. A* **1999**, *103*, 5935.

(42) Acetonitrile used as the solvent for the photochemical reaction via photoinduced electron transfer may be coordinated to Fe in coordinatively unsaturated intermediates in Scheme 2.

(43) The photoreduction of $[CpFe(CO)_2]_2$ by $(BNA)_2$ may also proceed via photoinduced electron transfer from $^3(BNA)_2$* to the unbridged trans isomer, which exists as a much less stable form, leading to facile Fe−Fe bond cleavage in the dimer radical anion. If this is the major pathway, the rate constant ($k_{obs} = K_{obs}\tau_T^{-1}$) derived from the dependence of Φ on $[Fp_2]$ (eq 2) would be much smaller than the rate constant of the photoinduced electron transfer determined directly from the appearance of the transient absorption at 470 nm due to $[CpFe(CO)_2]_2^{\bullet-}$ (Figure 7b). The agreement between the k_{obs} and k_{et} values obtained in this study indicates that a reaction pathway via a cleavage precursor such as an unbridged isomer of $[CpFe(CO)_2]_2$ is not a major pathway in the photoreduction of $[CpFe(CO)_2]_2$ by $(BNA)_2$.